JOURNAL OF CHEMICAL INFORMATION AND MODELING

Article

pubs.acs.org/jcim

# Autoinhibitory Mechanism for the Mutation-Induced Impaired FGF9 Signaling

Ying Wang,[†,‡] Xiao-Lin Wu,*[,§] Dong-Qing Wei,*[,‡] Yi-Xue Li,[∥,⊥] and Jing-Fang Wang*[,†,⊥]

[†]Key Laboratory of Systems Biomedicine (Ministry of Education), Shanghai Center for Systems Biomedicine, Shanghai Jiao Tong University, Shanghai 200240, China

[‡]State Key Laboratory of Microbial Metabolism and Department of Bioinformatics and Biostatistics, College of Life Science and Biotechnology, Shanghai Jiao Tong University, Shanghai 200240, China

[§]Department of Medical Genetics, Shanghai Jiao Tong University School of Medicine (SJTUSM), Shanghai 200025, China

[∥]Key Laboratory of Systems Biology, Shanghai Institutes for Biological Sciences, Chinese Academy of Science, Shanghai 200031, China

[⊥]Shanghai Center for Bioinformation Technology, 100 Qinzhou Road, Shanghai 200235, China

**ABSTRACT:** Fibroblast growth factor 9 (FGF9), an important member of the fibroblast growth factor (FGF) family, can bind with high affinity to FGFR3 in a heparin-dependent approach. In humans, the deletions and mutations resulting in dysfunction of the FGF9 signaling can cause human skeletal dysplasia and cancers. A mutation (S99N) in this protein has been identified to be associated with significantly impaired FGF signaling considered as a potential cause of synostoses syndrome. However, the detailed mechanism for this observation still remains unknown. In this study, we used molecular dynamics simulations and free energy calculations to study the interactions of $FGF9^{WT/S99N}$, FGFR3c, and heparin, with an aim of providing atomic sights into the detailed mechanism for the impaired FGF signaling caused by the S99N mutation. We found that the S99N mutation has a well-ordered C-terminal structure, which can reduce its homodimerization ability so as to break the monomer−dimer equilibrium in the FGF signaling, which is considered as a key factor to regulate extracellular matrix affinity and tissue diffusion in the FGF signaling pathway. The $FGF9^{WT}$ monomer can preferentially form a homodimer owing to its comparatively favorable binding free energy. In contrast, the $FGF9^{S99N}$ monomer is preferred to bind with the FGFR3c receptor to form an inactive complex, leading to impair FGF signaling. To support our computational findings, we also performed biochemical experiments, which confirm the computational results mentioned above. The impaired FGF signaling is believed to be a potential cause of human synostoses syndrome, implicating an important role for FGF9 in normal joint development.

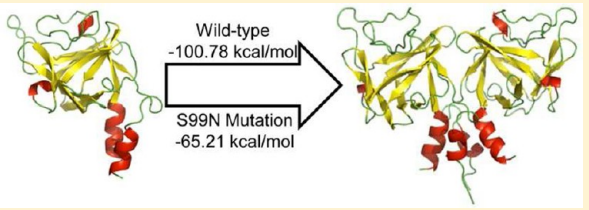


## INTRODUCTION

The fibroblast growth factors (FGFs) are a large family of polypeptide growth factors identified in the organisms ranging from nematodes to humans.[1,2] These proteins are widely expressed in developing and adult tissues and have diverse functions in organogenesis, tissue repair, nervous system control, metabolism, and physiological homeostasis.[3−5] In the embryonic development, FGF proteins function as a regulator for cellular proliferation, differentiation, and migration. In the adult, these proteins act as homeostatic factors in tissue repair and wound healing, in the control of the nervous system, and in tumor angiogenesis.[6] In humans and mice, the FGF proteins play crucial roles in numerous physiological and pathological processes through combining with FGF receptors (FGFR) composed of at least 8 members.[7] FGFR activation and signaling are dependent on FGFs induced dimerization, a process that also requires cell surface heparin or heparin sulfate proteoglycans.[8−10] Additional studies showed that heparin and/or heparin sulfate act to increase the affinity and half-life of the FGF-FGFR complex. Furthermore, many cancers and genetic diseases are associated with mutations in the expression and signaling activities of these ligands.[11−13] Consequently, FGFs and FGFRs as well as heparin (or heparin sulfates) are of primary importance in investigating human development and diseases.

Fibroblast growth factor 9 (FGF9), an important member of the FGF family, was originally discovered as a heparin-binding glia-activating factor. This protein employs nearly 30% sequence similarity with prototypical FGF family members FGF1 and FGF2. However, unlike FGF1 and FGF2, FGF9 has no effect on human umbilical vein endothelial cells, suggesting that this protein may have unique receptor specificity.[14] Additional evidence shows that the recombinant FGF9 can bind with high affinity to FGFR3 in a heparin-dependent approach so as to activate FGFR3. The activated FGFR3 can inhibit the proliferation of chondrocytes and endochondral ossification during ossature growth and damage.[15,16] Addition-

**Received:** June 29, 2012
**Published:** August 25, 2012





dx.doi.org/10.1021/ci3003045 | J. Chem. Inf. Model. 2012, 52, 2422−2429

ally, 6 distinct FGF9 mutations, including 1 frameshift, 4 missenses, and 1 nonsense, have been detected in human cancers.[17] In mice, deletion of this gene can also lead to skeletal dysplasias,[18] lung hypoplasis,[19] and male-to-female sex reversal.[20] Thus, it is believed that the deletion and mutations resulting in dysfunction of FGF9 signaling can cause human skeletal dysplasia and cancers.

A previous work showed that 12 affected patients with multiple synostoses syndrome in a large Chinese family have the exact mutation (S99N) in the FGF9 gene.[21] Further biochemical analysis revealed that this mutation is associated with significantly impaired FGF signaling and considered as a potential cause of synostoses syndrome, implicating an important role for FGF9 in normal joint development.[21] However, the detailed mechanism for the mutation S99N in FGF9 to impair the FGF signaling is still unknown. With an aim of understanding the structural basis for the impaired FGF signaling caused by the S99N mutation in the FGF9 gene, we employed molecular modeling and molecular dynamics simulations as well as free energy calculations to study the wild-type and mutated FGF9 and their complexes with FGFR3c and heparin. Such computational methods can provide timely information for both basic research and drug design,[22−27] greatly stimulating the development of the related areas.[28,29] Besides, further biochemical experiments were also performed to support the computational findings.

## METHODS AND COMPUTATIONAL DETAILS

**Structural Models.** The three-dimensional structures of the wild-type FGF9 ($FGF9^{WT}$) and FGFR3c monomers were taken from the Protein Data Bank (PDB) with PDB entries 1ihk.pdb[30] and 1ry7.pdb,[31] respectively. The monomer structure of the FGF9 S99N mutation ($FGF9^{S99N}$) was then constructed using the homology model procedure in Molecular Operating Environment (MOE) with the wild-type monomer structure (1ihk.pdb) as a structure template. Based on these monomer structures ($FGF9^{WT}$and $FGF9^{S99N}$), the dimeric structures for $FGF9^{WT}$ and $FGF9^{S99N}$ were built by the interactive protein docking program HEX,[32] which was also used to construct the complexes of $FGF9^{WT}$ -FGFR3c, $FGF9^{S99N}$-FGFR3c, dimer $FGF9^{WT}$ -FGFR3c, and dimer $FGF9^{S99N}$-FGFR3c. The structure of hexasasaccharide (UAP-SGN-IDU-SGN-IDU-SGN) from the PDB database is used as a heparin oligosaccharide. Using molecular docking program AutoDock Vina,[33−36] the heparin molecule was docking into both monomeric and dimeric structures of $FGF9^{WT}$ and $FGF9^{S99N}$.

**Molecular Dynamics Simulation.** The protein atoms in all the systems were parametrized by AMBER force field parameters. The force field parameters for heparin molecule were obtained from the antechamber package in AMBER 9.0,[37] which is a set of auxiliary programs for molecular mechanic studies. All the systems were solvated in a simulated box with ∼31880 explicit TIP3p water molecules. To neutralize the systems, 4 chloride ions were added for the monomer systems, and 8 chloride ions were added for the dimer systems to randomly place the equal number of water molecules. All the systems were then subjected to a steepest descent energy minimization (∼5000 steps), followed by conjugate gradient for the next 5000 steps, and subsequently equilibrated with FGF9, FGFR3c, and heparin atoms fixed by 1-ns molecular dynamics (MD) simulation to reduce the van der Waals conflicts. Finally, 10 ns MD simulations for all the systems were performed under the normal temperature (300 K) by the AMBER 9.0 package[37] with the periodic boundary conditions and NPT ensembles. During our MD simulations, the SHAKE algorithm with a tolerance of $10^{-6}$ was applied to constrain all bonds in the systems involving hydrogen atoms, and atoms velocities for start-up runs were obtained according to the Maxwell distribution at 300 K. The isothermal compressibility was set to $4.5 \times 10^{-5}$/bar for solvent simulations. The electrostatic interactions were treated by PME algorithm with interpolation order of 4 and a grid spacing of 0.12 nm. The van der Waals interactions were calculated by using a cutoff of 12 Å. All the MD simulations were performed with a time step of 1 fs, and coordinates were saved every 1 ps. For the statistic analyses, each MD trajectory has been repeated 10 times with the same starting structure and different atom velocities.

**Free Energy Calculation.** The molecular mechanics generalized Born surface area (MM-GB/SA) approach implemented in AMBER 9.0 was applied to calculate the binding free energy for all the simulated systems involved in our MD simulations. The principle of the MM-GB/SA method can be summarized as follows

$$\Delta G_{bind} = G_{complex} - (G_{protein} + G_{ligand}) \quad (1)$$

$$G \cong E_{gas} - TS_{config} + G_{sol} \quad (2)$$

$$E_{gas} = E_{bond} + E_{angle} + E_{torsion} + E_{vdw} + E_{ele} \quad (3)$$

$$G_{sol} = G_{ele} + G_{nonpolar} \quad (4)$$

In eq 1, the binding free energy change in protein−ligand binding ($\Delta G$) is calculated as the difference between the free energies of the complex ($G_{complex}$), the protein ($G_{protein}$), and the ligand ($G_{ligand}$). The free energies of the complex, the protein, and the ligand are computed through eq 2 by summing up its internal energy in the gas phase ($E_{gas}$), the solvation free energy ($G_{sol}$), and a vibrational entropy term ($TS$). $E_{gas}$ is a standard force field energy calculated from eq 3 by the strain energies from covalent bonds ($E_{bond}$ and $E_{angle}$) and torsion angles ($E_{torsion}$), noncovalent van der Waals ($E_{vdw}$), and electrostatic energies ($E_{ele}$). As described in eq 4, the solvation free energy ($G_{sol}$) is computed by both an electrostatic term ($G_{ele}$) and a nonpolar component ($G_{nonpolar}$). The former can be obtained from the Generalized Born (GB) method. The latter is considered to be proportional to the molecular solvent accessible surface area (SASA). In our study, 100 snapshots retrieved from the last 0.5-ns segment on the MD trajectories with an interval of 5 ps were used for the binding free energy calculations.

**Cell Culture and DNA Transfection.** COS-7 cells[38] were grown in Dulbecco's modified Eagle's medium (DMEM) containing 10% fetal calf serum. The cells were transiently transfected with different plasmid DNA constructs (contain FLAG-$FGF9^{WT}$ or FLAG-$FGF9^{S99N}$) using LipofectAMINE 2000 according to the manufacturer's instructions (Invitrogene). Cell lysate and culture supernatant were subjected to Western blot analysis and proliferation assay.

**Western Blot Analysis.** After transfected with $FGF9^{WT}$and $FGF9^{S99N}$ DNA constructs, cell extracts were prepared by lysis in RIPA buffer (50 mM Tris-HCl, pH 7.5, 150 mM NaCl, 1% deoxycholate, 0.1% SDS, 1% Nonidet P-40) at 4 °C for 30 min. Culture supernatant of DNA-transfected COS cells (mock transfected and with 10ug of DNA) from one 6-cm dish were incubated with heparin-Sepharose beads overnight at 4 °C. The


dx.doi.org/10.1021/ci3003045 | J. Chem. Inf. Model. 2012, 52, 2422−2429

beads were washed twice with phosphate-buffered saline (PBS) and suspended in Laemmli buffer. The eluted proteins were separated by SDS-PAGE (12.5% gels) and transferred onto nitrocellulose membranes. After blocking with 5% fat-free milk powder in PBS, the membranes were incubated overnight with the anti-FGF9 antibodies at 4 °C. The bound antibodies revealed with IRDyeTM800CWConjugated Affinity Purified Antirabbit IgG.

**Proliferation Assay.** The RCJ3.1C5.18 chondrocyte cell line[21] was grown in conditional medium containing normal complete medium ($\alpha$-MEM supplemented with 15% heat-inactivated fetal bovine serum, $10^{-7}$ M dexamethasone, and 2 mM sodium pyruvate) and transfected cell cultured medium (volume 1:1). Cells were plated at a density of $6 \times 10^4$ cells/well in six-well dishes. After reaching confluence, cells were further cultured with the presence of 50 mg/mL ascorbic acid phosphate, 10 mM -glycerophosphate (Sigma), and heparin (2 mg/mL). Cells were counted at day 4 and day 7.

## RESULTS AND DISCUSSION

**$FGF9^{WT}$ Complexes in the Natural FGF Signaling Pathway.** As a typical member of the FGF family, FGF9 adopts a $\beta$-trefoil folding structure (Figure 1A). The core unit

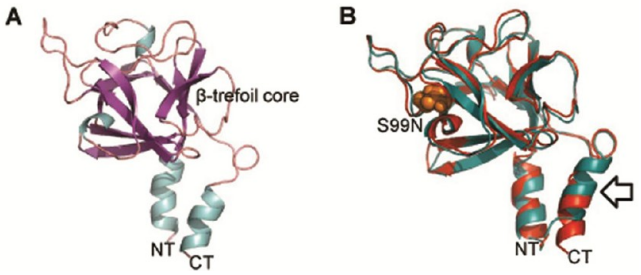


**Figure 1.** Ribbon diagram of $FGF9^{WT/S99N}$. (A) The backbone structure of $FGF9^{WT}$. $\alpha$ helices, $\beta$ strands, and loop regions are colored in light blue, purple, and pink respectively. NT and CT denote the N- and C-terminal. (B) The structural comparison of $FGF9^{WT/S99N}$. The backbone structures of $FGF9^{WT/S99N}$ are colored in red and green respectively. S99N mutation is labeled in orange space-filling representations. The black arrow shows the significant difference between $FGF9^{WT/S99N}$.

of the wild-type FGF9 ($FGF9^{WT}$) is formed by the residues 62−193. This part of the structure is very similar with the prototypical FGF members FGF1 and FGF2. According to the crystal studies, the root-mean-square (rms) difference of the C$\alpha$ atoms in this part with that of FGF1 and FGF2 is about 1.0 Å and 0.73 Å, respectively.[37] The regions with rms deviation values >1.5 Å are mainly located on the residues 88−90, 141−146, and 153−161. These regions are correlated with the C-terminal extension in FGF9 and mainly form flexible loop structures. As the S99N mutation in FGF9 ($FGF9^{S99N}$) is far away from the $\beta$-trefoil, it is not expected to have huge alterations on the overall structures of the protein (Figure 1B). Superposition of the C$\alpha$ trances of the mutant structure with those of the wild-type gives a rms deviation of ∼1.43 Å. The significant structural differences between the $FGF9^{WT}$ and $FGF9^{S99N}$ structures are detected in the 3−10 helix near C-terminal extension. The hydrogen bonding network in this region is quite different in the wild and mutated systems (Table 1). The hydrogen bonds in the C-terminal region of the $FGF9^{S99N}$ structure are much stronger than those of the

**Table 1. Hydrogen Bonding Network near the C-Terminal Region**

| systems | donor | receptor | distance (Å) | occupancy |
|---|---|---|---|---|
| $FGF9^{WT}$ | Glu199 | Lys202 | 3.03 ± 0.61 | 12.7% |
| | Leu200 | Ile204 | 3.04 ± 0.67 | 18.3% |
| | Tyr201 | Leu205 | 2.93 ± 0.49 | 50.1% |
| | Lys202 | Ser206 | 3.19 ± 0.80 | 32.7% |
| | Ile204 | Gln207 | 3.38 ± 0.99 | 14.3% |
| | Ile204 | Ser208 | 3.24 ± 0.94 | 17.1% |
| $FGF9^{S99N}$ | Val197 | Tyr201 | 3.24 ± 0.92 | 23.8% |
| | Pro198 | Lys202 | 3.43 ± 1.15 | 12.1% |
| | Tyr201 | Leu205 | 3.09 ± 0.70 | 39.5% |
| | Tyr201 | Ile204 | 2.97 ± 0.52 | 30.4% |
| | Lys202 | Ser206 | 3.13 ± 0.76 | 34.6% |
| | Asp203 | Gln207 | 2.63 ± 0.37 | 33.9% |
| | Gln207 | Ser208 | 2.12 ± 0.28 | 47.8% |

$FGF9^{WT}$ structure for their higher occupancies and shorter bond distances. The stronger hydrogen bonds in the $FGF9^{S99N}$ structure can maintain the 3−10 helix in a better ordered-structure than that of the $FGF9^{WT}$ structure. However, this helix is located on the dimer interface according to the crystal reports, and an incompact structure is preferred for the dimer formation. So, the well ordered-structure in the 3−10 helix of the $FGF9^{S99N}$ structure may be not propitious for the dimer formation of FGF9 in the natural FGF signaling pathway.

The wild-type FGF9 ($FGF9^{WT}$) monomer can form 3 complexes ($FGF9^{WT}$-FGFR3c, $FGF9^{WT}$-heparin, and the $FGF9^{WT}$ dimer) with FGFR3c, heparin, or itself in the physiological environment. To determine which complex the $FGF9^{WT}$ monomer preferentially forms, we calculated the binding free energies for these complexes (Figure 2, for detailed information please see Table 2). Owing to the favorable binding free energy (−100.78 ± 10.23 kcal/mol), which is much higher in magnitude than those to form $FGF9^{WT}$-heparin (−19.61 ± 6.47 kcal/mol) and $FGF9^{WT}$-FGFR3c (−64.33 ±

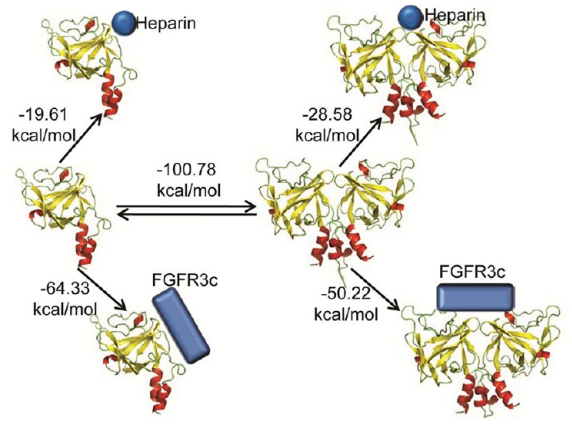


**Figure 2.** Schematic showing the binding free energies (kcal/mol) for the complexes in the $FGF9^{WT}$ system. In the natural FGF signaling, the wild-type FGF9 ($FGF9^{WT}$) can form 3 complexes: $FGF9^{WT}$-heparin ($\Delta G_{bind}$ = −19.61 ± 6.47 kcal/mol), $FGF9^{WT}$-FGFR3c ($\Delta G_{bind}$ = −64.33 ± 9.72 kcal/mol), and the $FGF9^{WT}$ homodimer ($\Delta G_{bind}$ = −100.78 ± 10.23 kcal/mol). The $FGF9^{WT}$ dimer preferentially binds the FGFR3c receptor ($\Delta G_{bind}$ = −50.22 ± 17.78 kcal/mol) rather than heparin ($\Delta G_{bind}$ = −28.58 ± 11.27 kcal/mol), and the dimer $FGF9^{WT}$-FGFR3c-heparin can induce the normal FGF signaling.


dx.doi.org/10.1021/ci3003045 | J. Chem. Inf. Model. 2012, 52, 2422−2429

Table 2. Binding Free Energies (kcal/mol) for Both FGF9$^{WT}$ and FGF9$^{S99N}$ Systems[a]

| | $\Delta E_{vdw}$ | $\Delta G_{nonpolar}$ | $\Delta G_{ele}$ | $\Delta G_{binding}$ |
|---|---|---|---|---|
| FGF9$^{WT}$-heparin | −41.22 ± 7.74 | −6.21 ± 0.80 | 27.82 ± 7.34 | −19.61 ± 6.47 |
| FGF9$^{WT}$-FGFR3c | −119.20 ± 7.53 | −18.52 ± 1.00 | 73.38 ± 9.33 | −64.33 ± 9.72 |
| FGF9$^{S99N}$-heparin | −55.05 ± 4.57 | −7.23 ± 0.43 | 30.18 ± 5.12 | −32.10 ± 5.98 |
| FGF9$^{S99N}$-FGFR3c | −147.71 ± 12.58 | −22.15 ± 1.30 | 74.95 ± 12.87 | −94.89 ± 8.73 |
| dimeric FGF9$^{WT}$-heparin | −54.52 ± 7.04 | −7.83 ± 0.50 | 33.77 ± 7.66 | −28.58 ± 11.27 |
| dimeric FGF9$^{WT}$-FGFR3c | −133.51 ± 14.85 | −22.06 ± 2.11 | 105.33 ± 9.43 | −50.22 ± 17.78 |
| dimeric FGF9$^{S99N}$-heparin | −64.72 ± 25.80 | −9.31 ± 0.47 | 21.72 ± 13.58 | −50.23 ± 12.05 |
| dimeric FGF9$^{S99N}$-FGFR3c | −83.64 ± 13.00 | −17.18 ± 2.13 | 74.16 ± 8.54 | −26.65 ± 11.15 |

[a] $\Delta E_{vdw}$: noncovalent van der Waals contributions from molecular mechanics; $\Delta G_{nonpolar}$: nonpolar component of the solvation free energy; $\Delta G_{ele}$: electrostatic term calculated from the Generalized Born (GB) method; $\Delta G_{binding}$: binding free energy.

9.72 kcal/mol) complexes, the FGF9$^{WT}$ monomer is preferred to be dimerization. This is also supported by the sedimentation equilibrium analytical ultracentrifugation studies that the FGF9 dimerization has a $K_d$ constant of 680 nM.[37] This monomer−dimer equilibration is also reported to have significant influence on the FGF signaling pathway.[8] After forming a homodimer, the FGF9$^{WT}$ dimer structure binds to FGFR3c to form a dimer FGF9$^{WT}$-FGFR3c complex with a much more favorable binding free energy (−50.22 ± 17.78 kcal/mol) than that of the dimer FGF9$^{WT}$-heparin complex (−28.58 ± 11.27 kcal/mol). By such a way, the wild-type FGF9 (FGF9$^{WT}$) can achieve its biological functions by forming the active complexes in a two-end model, leading to the natural FGF signaling.

**FGF9$^{S99N}$ Mutated Complex in the Impaired FGF Signaling Pathway.** Although the FGF9$^{S99N}$ has a very similar overall structure with the wild-type structure, the 3−10 helix in the FGF9$^{S99N}$ structure is well ordered than that of the wild-type structure (FGF9$^{WT}$). In the crystal structure, this helix is located near the homodimer interface and is thought to be composed of two major parts: an interface part inside the $\beta$-trefoil core or an interface part outside the $\beta$-trefoil core (Figure 3). The former mainly involves in the $\beta$1, $\beta$2 strands and $\beta$8-$\beta$9 loops, the latter contains $\alpha$ helices in both N- and C-terminals, and the loops connecting these helices to the $\beta$-trefoil core. However, due to employing significant hydrophobic contacts with the adjacent FGF9 monomer, the interface outside the $\beta$-trefoil core has major contributions to the FGF9 dimerization. Besides the hydrophobic contacts, some hydrogen bonds (such as the ones between the side chains of Tyr64 and Asn143, the side chain of Arg64, and the backbone carbonyl group of Val192) and salt bridges (such as the one between Arg62 and Asp193) are also detected in this interface. The well-ordered 3−10 helix in the FGF9$^{S99N}$ structure may break these hydrophobic contacts, hydrogen bonds, or salt bridges, so as to reduce the dimerization ability.

This point is further proved by the free energy calculations for the FGF9$^{S99N}$ systems. The binding free energy for the FGF9$^{S99N}$ homodimer is −65.21 ± 8.96 kcal/mol (Figure 4, for detailed information please see Table 2), much less favorable than that of the FGF9$^{WT}$ homodimer (−100.78 ± 10.23 kcal/mol), indicating that FGF9$^{S99N}$ has poor ability to homodimerize. In such a case, the FGF9$^{S99N}$ structure should be preferred to bind with FGFR3c due to the comparatively favorable binding free energy (−94.89 ± 8.73 kcal/mol). However, homodimerization is believed to be a common feature of FGF proteins, such as FGF2, FGF9, FGF16, and FGF20.[6] The monomer−dimer equilibrium in FGF9$^{WT}$ is

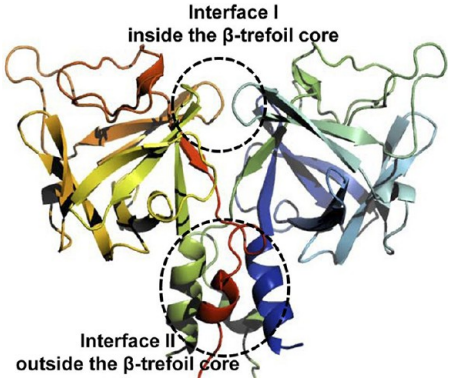


Figure 3. The dimer interface regions in the wild-type FGF9. The dimer interface regions can be divided into two major parts based on their locations: inside or outside the $\beta$-trefoil core. The interface inside the $\beta$-trefoil core involves in the $\beta$1, $\beta$2 strands and $\beta$8-$\beta$9 loops; the one outside the $\beta$-trefoil core contains the helices in both N- and C-terminals, and the loops connecting these helices to the $\beta$-trefoil core.

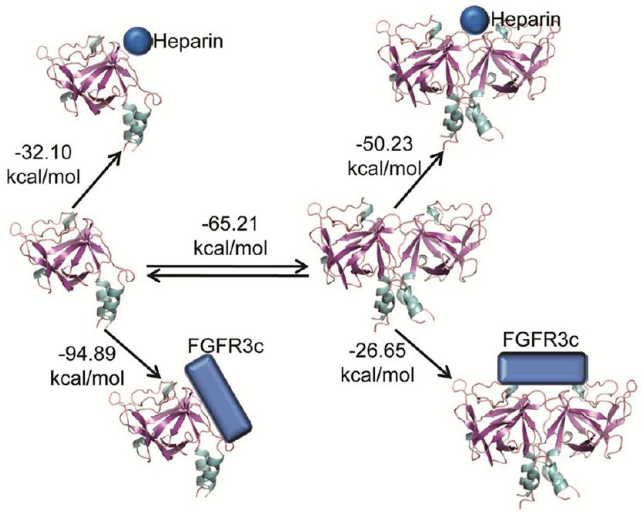


Figure 4. Schematic showing the binding free energies (kcal/mol) for the complexes in the FGF9$^{S99N}$ system. In the impaired FGF signaling, the S99N mutation (FGF9$^{S99N}$) can form 3 complexes: FGF9$^{S99N}$-heparin ($\Delta G_{bind}$ = −30.21 ± 5.98 kcal/mol), FGF9$^{S99N}$-FGFR3c ($\Delta G_{bind}$ = −94.89 ± 8.73 kcal/mol), and the FGF9$^{S99N}$ homodimer ($\Delta G_{bind}$ = −65.21 ± 8.96 kcal/mol). The poor dimerization ability reduces the binding affinities for both FGF9$^{S99N}$-FGFR3c ($\Delta G_{bind}$ = −26.65 ± 11.15 kcal/mol) and FGF9$^{S99N}$-heparin ($\Delta G_{bind}$ = −50.23 ± 12.05 kcal/mol), resulting in an inactive FGF9$^{S99N}$-FGFR3c-heparin to induce an impaired FGF signaling.


dx.doi.org/10.1021/ci3003045 | J. Chem. Inf. Model. 2012, 52, 2422−2429

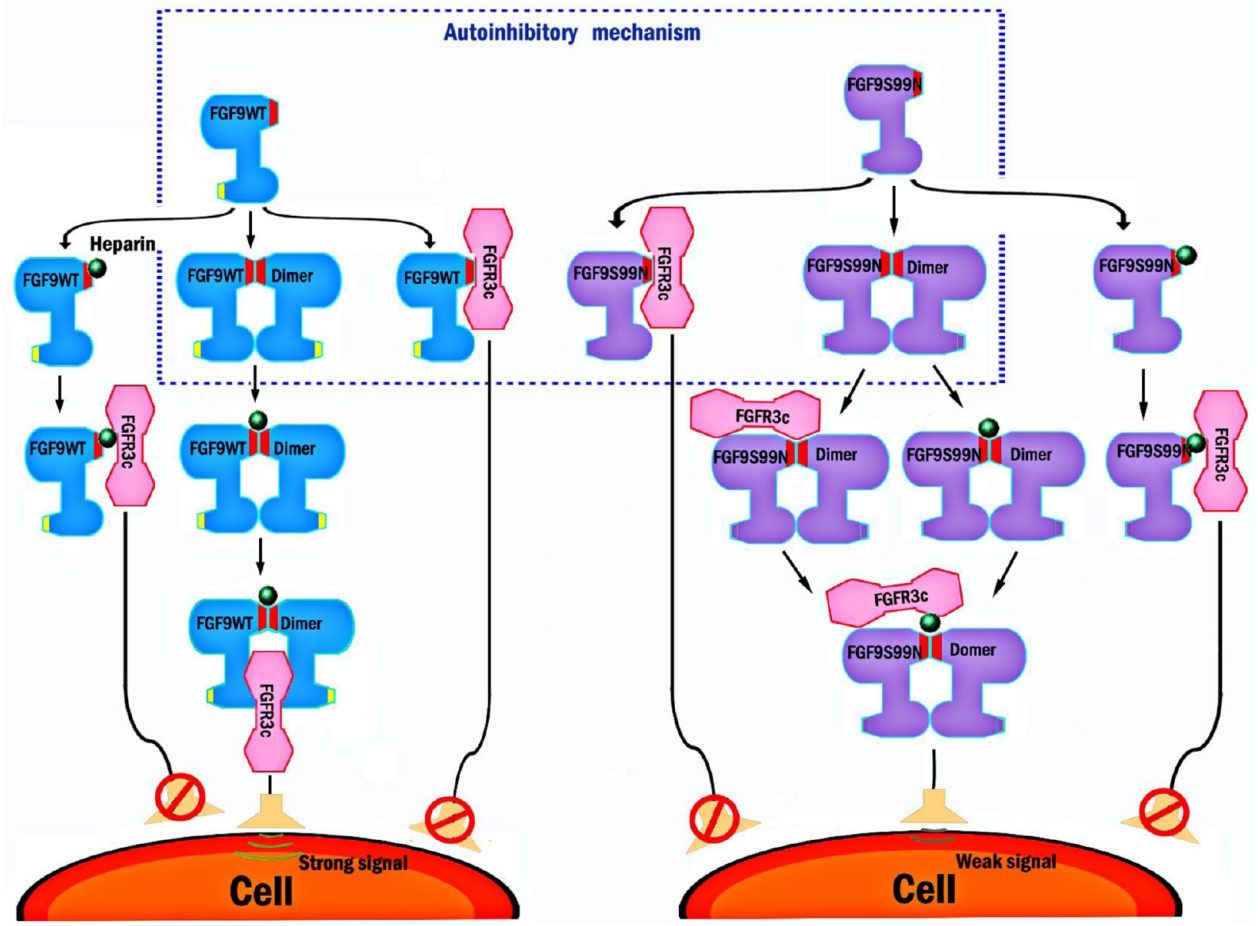


**Figure 5.** Autoinhibitory mechanism for both $FGF9^{WT}$ and $FGF9^{S99N}$ systems. In the wild-type FGF9 system, the normal signal is generated by the active complex dimer $FGF9^{WT}$-FGFR3c-heparin. However, the $FGF9^{WT}$ monomer can also form $FGF9^{WT}$-FGFR3c and $FGF9^{WT}$-heparin before its dimerization, which are inactive complexes and induce an impaired and weak signal in the FGF signaling pathway. In the S99N mutated system, due to the poor dimerization ability all the complexes are inactive, inducing an impaired and weak signal in the FGF signaling pathway.

further proved to play an important role of regulating extracellular matrix affinity and tissue diffusion in the FGF signaling pathway.[8−10] A stable homodimer structure is the principal factor for FGF9 to induce FGFR3c activation. Due to the poor ability to homodimerize, the $FGF9^{S99N}$ dimer structure also employs a more favorable binding affinity with FGFR3c. The binding free energy for the dimer $FGF9^{S99N}$-FGFR3c complex is about $-26.65 \pm 11.15$ kcal/mol, less favorable than that of the dimer FGF9WT-FGFR3c complex ($-50.22 \pm 17.78$ kcal/mol). Interestingly, from the simulation trajectories of the dimer $FGF9^{WT/S99N}$-FGFR3c complexes, we find that the receptor binding sites in the wild-type and mutant dimeric structures are different. In the $FGF9^{WT}$ dimer structure, FGFR3c binds outside of the $\beta$-trefoil core, near the N- and C-terminal regions, to form a two-end model. This model has been demonstrated by crystal studies to be essential for the FGF signaling.[39,40] In the two-end model, the free energy for heparin to bind to the dimer $FGF9^{WT}$-FGFR3c complex is $-30.12 \pm 11.25$ kcal/mol. In the $FGF9^{S99N}$ dimer structure, the receptor binds near the $\beta$-trefoil core, which is an inactive complex and cannot fit the two-end model. In the dimer FGF9S99N-FGFR3c complex, the binding free energy for heparin is $18.79 \pm 7.61$ kcal/mol, much less favorable than that of the dimer $FGF9^{WT}$-FGFR3c complex mentioned above.

**Autoinhibitory Mechanism.** According to the structural and energetic analyses mentioned above, detailed descriptions for the active complexes in the natural FGF signaling pathway can be obtained, and an autoinhibitory mechanism can be summarized (Figure 5). In the natural FGF signaling, the wild-type FGF9 ($FGF9^{WT}$) can form 3 biological complexes: $FGF9^{WT}$- heparin ($\Delta G_{bind} = -19.61 \pm 6.47$ kcal/mol), $FGF9^{WT}$-FGFR3c ($\Delta G_{bind} = -64.33 \pm 9.72$ kcal/mol), and the $FGF9^{WT}$ homodimer ($\Delta G_{bind} = -100.78 \pm 10.23$ kcal/mol). $FGF9^{WT}$- heparin and $FGF9^{WT}$-FGFR3c can further bind FGFR3c and heparin respectively to form the inactive complex $FGF9^{WT}$-FGFR3c-heparin. This complex cannot successfully activate the FGF receptor FGFR3c so as to induce an impaired and weak signal in the FGF signaling pathway. However, in the physiological environment most of the wild-type FGF9 ($FGF9^{WT}$) proteins will preferentially form homodimers, which is essential for the FGF receptor activation. The homodimer will further bind with FGFR3c to dimer $FGF9^{WT}$-FGFR3c ($\Delta G_{bind} = -50.22 \pm 17.78$ kcal/mol), subsequently binding heparin to form an active complex dimer $FGF9^{WT}$-FGFR3c-heparin. The active complex dimer $FGF9^{WT}$-FGFR3c-heparin can provide a correct and strong signal to induce the natural FGF signaling pathway. Thus, the monomer−dimer equilibrium of the wild-type FGF9 ($FGF9^{WT}$) system is believed to be primary for the active complex dimer $FGF9^{WT}$-FGFR3c-heparin formation and for the normal signal in the natural FGF signaling pathway.


dx.doi.org/10.1021/ci3003045 | J. Chem. Inf. Model. 2012, 52, 2422−2429

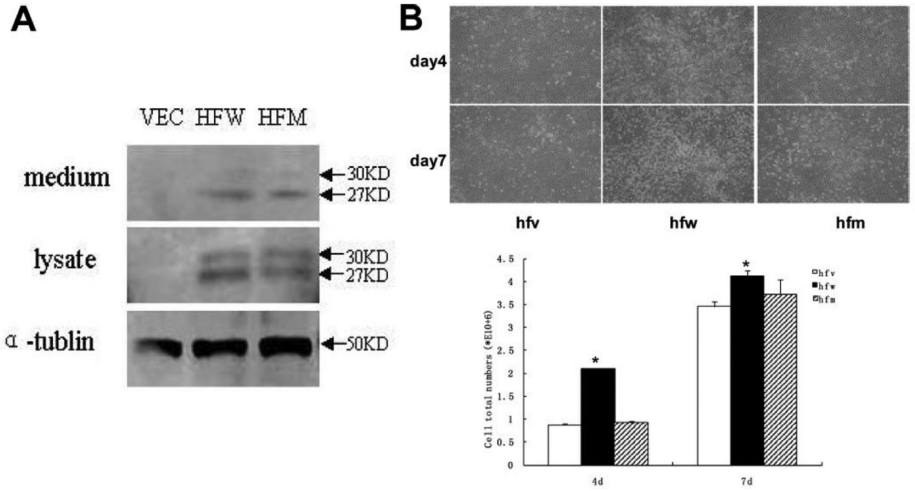


**Figure 6.** Experimental validation of the wild-type and S99N mutated FGF9. (A) Western blotting analysis of both wild-type (HFW) and S99N mutated (HFM) FGF9, which gives an indication that the S99N mutation has no effect on FGF9 protein secretion. (B) Wild-type and mutated FGF9 proliferation analysis, indicating that the S99N mutation can reduce the binding affinity to FGFR3c and induce an impaired FGF signal.

In the $FGF9^{S99N}$ system, the mutated FGF9 ($FGF9^{S99N}$) structure can also form 3 complexes: $FGF9^{S99N}$-heparin ($\Delta G_{bind}$ = −30.21 ± 5.98 kcal/mol), $FGF9^{S99N}$-FGFR3c ($\Delta G_{bind}$ = −94.89 ± 8.73 kcal/mol), and the $FGF9^{S99N}$ homodimer ($\Delta G_{bind}$ = −65.21 ± 8.96 kcal/mol). Different from the wild-type system, most of the $FGF9^{S99N}$ monomer will select to bind the FGF receptor FGFR3c to form $FGF9^{S99N}$-FGFR3c. According to the previous analyses, the complexes $FGF9^{S99N}$-heparin and $FGF9^{S99N}$-FGFR3c cannot activate the FGF receptor, leading to an impaired and weak signal in the FGF signaling pathway. After dimerization, the $FGF9^{S99N}$ homodimer is preferred to bind the important ligand heparin to form the dimer $FGF9^{S99N}$-heparin complex ($\Delta G_{bind}$ = −52.30 ± 12.05 kcal/mol), subsequently forming the complex dimer $FGF9^{S99N}$-FGFR3c-heparin. The $FGF9^{S99N}$ homodimer can also bind the FGF receptor FGFR3c to form the complex dimer $FGF9^{S99N}$-FGFR3c, but the binding affinity is less favorable ($\Delta G_{bind}$ = −26.65 ± 11.15 kcal/mol). The inactive complex dimer $FGF9^{S99N}$-FGFR3c-heparin formed by both dimer $FGF9^{S99N}$-heparin and dimer $FGF9^{S99N}$-FGFR3c cannot induce the normal signal in the natural FGF signaling pathway. These complexes can only provide an impaired and weak signaling.

**Experimental Validation.** To give experimental support, we also performed experimental validations. COS-7 cells were transiently transfected with both wild-type and S99N mutant FGF9 expression plasmid DNA. Cell lysate and culture medium were subjected to Western blotting analysis after 48 h (Figure 6A). The results show no differences between wild-type and S99N mutant FGF9 proteins secreted in the medium, giving an indication that the S99N mutation has no effect on FGF9 protein secretion. To analyze the cell growth, RCJ3.1C5.18 cells are plated at 6 × 104 in each of the 6-well plates. The viable cells are counted at day 4 and day 7 and compared to the control. As shown in Figure 6B, $FGF9^{WT}$ proteins (hfw) significantly promote the proliferation of RCJ 3.1C5.18 cartilage cells, but the mutant proteins (hfm) lost this capacity. Cell counts were performed using a hemocytomer. These results were reproduced three times; an * indicates a p value less than 0.05 (WT vs mutant). Thus, our study has supported that the existence of S99N mutation could impair the affinity between FGF9 and FGFR3c with resulting degraded function which is to promote chondrocytic rat cell proliferation.

## ■ CONCLUSION

Monomer−dimer equilibrium in human FGF9 is an essential factor for FGF signaling pathway, which can regulate extracellular matrix affinity and tissue diffusion in the FGF signaling pathway. Although the S99N mutation does not change the entire protein folding, it can reduce homodimerization ability of FGF9, breaking the important monomer−dimer equilibrium and forming inactive complexes with FGFR3c and heparin. Based on these findings, an autoinhibitory mechanism is proposed to explain why the substitution from serine to asparagines at position 99 can lead to the impaired FGF signaling. No matter in the wild-type or mutant system, the FGF9 monomer can bind heparin, FGFR3c, or itself to form a homodimer. In the wild-type system, due to more favorable binding free energy (−100.78 ± 10.23 kcal/mol), the $FGF9^{WT}$ monomer is preferred to form a homodimer that can further bind to heparin and FGFR3c, leading to normal signal conduction in FGF signaling. However, the $FGF9^{S99N}$ monomer in the mutant system is inclined to bind FGFR3c for the more favorable binding free energy (−94.89 ± 8.73 kcal/mol). The $FGF9^{S99N}$ monomer-FGFR3c complex cannot activate the FGF receptor FGFR3c causing an impaired FGF signaling. The impaired FGF signaling is believed to be a potential cause of human synostoses syndrome, implicating an important role for FGF9 in normal joint development.

## ■ AUTHOR INFORMATION

### Corresponding Author

*E-mail: wuxiaolin999@hotmail.com (X.L.-W.), dqwei@sjtu.edu.cn (D.Q.-W.), jfwang8113@sjtu.edu.cn (J.F.-W.).

### Notes

The authors declare no competing financial interest.

## ■ ACKNOWLEDGMENTS

This work was supported by the grants from National Basic Research Program of China (973 Program, 2011CB707500 and 2012CB721000), National High-Tech R Program (863 Program, No.2012AA020307), National Natural Science

Foundation of China (No. 30870476, 90913009, 81071444, and 31200547), Doctoral Program Foundation of Institutions of Higher Education of China (No. 20110073120078), China Postdoctoral Science Foundation (No. 20110490068), Shanghai Natural Science Foundation (No. 10ZR1417400), Key Project of Shanghai Science and Technology Commission (No. 11JC1406400), Innovation Program of Shanghai Municipal Education Commission (No. 09YZ95), and Chinese Academy of Sciences (KSCX2-YW-R-112).

## REFERENCES

(1) Gospodarowicz, D.; Jones, K. L.; Sato, G. Purification of a growth factor for ovarian cells from bovine pituitary glands. *Proc. Natl. Acad. Sci. U.S.A.* **1974**, *71*, 2295−2299.
(2) Cotton, L. M.; O'Bryan, M. K.; Hinton, B. T. Cellular signaling by fibroblast growth factors (FGFs) and their receptors (FGFRs) in male reproduction. *Endocr. Rev.* **2008**, *29*, 193−216.
(3) Basilico, C.; Moscatelli, D. The FGF family of growth factors and oncogenes. *Adv. Cancer Res.* **1992**, *59*, 115−165.
(4) Burgess, W. H.; Maciag, T. The heparin-binding (fibroblast) growth factor family of proteins. *Annu. Rev. Biochem.* **1989**, *58*, 575−606.
(5) Naski, M. C.; Ornitz, D. M. FGF signaling in skeletal development. *Front. Biosci.* **1998**, *3*, d781−94.
(6) Eswarakumar, V. P.; Lax, I.; Schlessinger, J. Cellular signaling by fibroblast growth factor receptors. *Cytokine Growth Factor Rev.* **2005**, *16*, 139−149.
(7) Galzie, Z.; Kinsella, A. R.; Smith, J. A. Fibroblast growth factors and their receptors. *Biochem. Cell. Biol.* **1997**, *75*, 669−685.
(8) Harada, M.; Murakami, H.; Okawa, A.; Okimoto, N.; Hiraoka, S.; Nakahara, T.; Akasaka, R.; Shiraishi, Y.; Futatsugi, N.; Mizutani-Koseki, Y.; Kuroiwa, A.; Shirouzu, M.; Yokoyama, S.; Taiji, M.; Iseki, S.; Ornitz, D. M.; Koseki, H. FGF9 monomer-dimer equilibrium regulates extracellular matrix affinity and tissue diffusion. *Nat. Genet.* **2009**, *41*, 289−298.
(9) Ornitz, D. M.; Itoh, N. Fibroblast growth factors. *Genome Biol.* **2001**, *2*, REVIEWS3005.
(10) Ornitz, D. M.; Yayon, A.; Flanagan, J. G.; Svahn, C. M.; Levi, E.; Leder, P. Heparin is required for cell-free binding of basic fibroblast growth factor to a soluble receptor and for mitogenesis in whole cells. *Mol. Cell. Biol.* **1992**, *12*, 240−247.
(11) Yayon, A.; Klagsbrun, M.; Esko, J. D.; Leder, P.; Ornitz, D. M. Cell surface, heparin-like molecules are required for binding of basic fibroblast growth factor to its high affinity receptor. *Cell* **1991**, *64*, 841−848.
(12) Plotnikov, A. N.; Hubbard, S. R.; Schlessinger, J.; Mohammadi, M. Crystal structures of two FGF-FGFR complexes reveal the determinants of ligand-receptor specificity. *Cell* **2000**, *101*, 413−424.
(13) Nybakken, K.; Perrimon, N. Heparan sulfate proteoglycan modulation of developmental signaling in Drosophila. *Biochim. Biophys. Acta* **2002**, *1573*, 280−291.
(14) Miyamoto, M.; Naruo, K.; Seko, C.; Matsumoto, S.; Kondo, T.; Kurokawa, T. Molecular cloning of a novel cytokine cDNA encoding the ninth member of the fibroblast growth factor family, which has a unique secretion property. *Mol. Cell. Biol.* **1993**, *13*, 4251−4259.
(15) Montero, A.; Okada, Y.; Tomita, M.; Ito, M.; Tsurukami, H.; Nakamura, T.; Doetschman, T.; Coffin, J. D.; Hurley, M. M. Disruption of the fibroblast growth factor-2 gene results in decreased bone mass and bone formation. *J. Clin. Invest.* **2000**, *105*, 1085−1093.
(16) Hung, I. H.; Yu, K.; Lavine, K. J.; Ornitz, D. M. FGF9 regulates early hypertrophic chondrocyte differentiation and skeletal vascularization in the developing stylopod. *Dev. Biol.* **2007**, *307*, 300−313.
(17) Abdel-Rahman, W. M.; Kalinina, J.; Shoman, S.; Eissa, S.; Ollikainen, M.; Elomaa, O.; Eliseenkova, A. V.; Butzow, R.; Mohammadi, M.; Peltomaki, P. Somatic FGF9 mutations in colorectal and endometrial carcinomas associated with membranous beta-catenin. *Hum. Mutat.* **2008**, *29*, 390−397.
(18) Ornitz, D. M.; Marie, P. J. FGF signaling pathways in endochondral and intramembranous bone development and human genetic disease. *Genes Dev.* **2002**, *16*, 1446−1465.
(19) Colvin, J. S.; White, A. C.; Pratt, S. J.; Ornitz, D. M. Lung hypoplasia and neonatal death in Fgf9-null mice identify this gene as an essential regulator of lung mesenchyme. *Development* **2001**, *128*, 2095−2106.
(20) Colvin, J. S.; Green, R. P.; Schmahl, J.; Capel, B.; Ornitz, D. M. Male-to-female sex reversal in mice lacking fibroblast growth factor 9. *Cell* **2001**, *104*, 875−889.
(21) Wu, X. L.; Gu, M. M.; Huang, L.; Liu, X. S.; Zhang, H. X.; Ding, X. Y.; Xu, J. Q.; Cui, B.; Wang, L.; Lu, S. Y.; Chen, X. Y.; Zhang, H. G.; Huang, W.; Yuan, W. T.; Yang, J. M.; Gu, Q.; Fei, J.; Chen, Z.; Yuan, Z. M.; Wang, Z. G. Multiple synostoses syndrome is due to a missense mutation in exon 2 of FGF9 gene. *Am. J. Hum. Genet.* **2009**, *85*, 53−63.
(22) Li, J.; Wei, D. Q.; Wang, J. F.; Li, Y. X. A negative cooperativity mechanism of human CYP2E1 inferred from molecular dynamics simulations and free energy calculations. *J. Chem. Inf. Model.* **2011**, *51*, 3217−3225.
(23) Wang, J. F.; Chou, K. C. Insights from modeling the 3D structure of New Delhi metallo-beta-lactamse and its binding interactions with antibiotic drugs. *PLoS One* **2011**, *6*, e18414.
(24) Lian, P.; Wei, D. Q.; Wang, J. F.; Chou, K. C. An allosteric mechanism inferred from molecular dynamics simulations on phospholamban pentamer in lipid membranes. *PLoS One* **2011**, *6*, e18587.
(25) Wang, J. F.; Hao, P.; Li, Y. X.; Dai, J. L.; Li, X. Exploration of conformational transition in the aryl-binding site of human FXa using molecular dynamics simulations. *J. Mol. Model.* **2012**, *18*, 2717−2725.
(26) Wang, Y.; Wei, D. Q.; Wang, J. F. Molecular dynamics studies on T1 lipase: insight into a double-flap mechanism. *J. Chem. Inf. Model.* **2010**, *50*, 875−878.
(27) Wang, J. F.; Chou, K. C. Insights into the mutation-induced HHH syndrome from modeling human mitochondrial ornithine transporter-1. *PLoS One* **2012**, *7*, e31048.
(28) Wang, J. F.; Chou, K. C. Molecular modeling of cytochrome P450 and drug metabolism. *Curr. Drug Metab.* **2010**, *11*, 342−346.
(29) Chen, Q.; Zhang, T.; Wang, J. F.; Wei, D. Q. Advances in human cytochrome p450 and personalized medicine. *Curr. Drug Metab.* **2011**, *12*, 436−444.
(30) Plotnikov, A. N.; Eliseenkova, A. V.; Ibrahimi, O. A.; Shriver, Z.; Sasisekharan, R.; Lemmon, M. A.; Mohammadi, M. Crystal structure of fibroblast growth factor 9 reveals regions implicated in dimerization and autoinhibition. *J. Biol. Chem.* **2001**, *276*, 4322−4329.
(31) Olsen, S. K.; Ibrahimi, O. A.; Raucci, A.; Zhang, F.; Eliseenkova, A. V.; Yayon, A.; Basilico, C.; Linhardt, R. J.; Schlessinger, J.; Mohammadi, M. Insights into the molecular basis for fibroblast growth factor receptor autoinhibition and ligand-binding promiscuity. *Proc. Natl. Acad. Sci. U.S.A.* **2004**, *101*, 935−940.
(32) Ritchie, D. W.; Venkatraman, V. Ultra-fast FFT protein docking on graphics processors. *Bioinformatics* **2010**, *26*, 2398−2405.
(33) Trott, O.; Olson, A. J. AutoDock Vina: improving the speed and accuracy of docking with a new scoring function, efficient optimization, and multithreading. *J. Comput. Chem.* **2010**, *31*, 455−461.
(34) Zeng, Q. K.; Du, H. L.; Wang, J. F.; Wei, D. Q.; Wang, X. N.; Li, Y. X.; Lin, Y. Reversal of coenzyme specificity and improvement of catalytic efficiency of Pichia stipitis xylose reductase by rational site-directed mutagenesis. *Biotechnol. Lett.* **2009**, *31*, 1025−1029.
(35) Wang, J. F.; Wei, D. Q.; Li, L.; Zheng, S. Y.; Li, Y. X.; Chou, K. C. 3D structure modeling of cytochrome P450 2C19 and its implication for personalized drug design. *Biochem. Biophys. Res. Commun.* **2007**, *355*, 513−519.
(36) Wang, J. F.; Wei, D. Q.; Chen, C.; Li, Y.; Chou, K. C. Molecular modeling of two CYP2C19 SNPs and its implications for personalized drug design. *Protein Pept. Lett.* **2008**, *15*, 27−32.
(37) Case, D. A.; Cheatham, T. E., III; Darden, T.; Gohlke, H.; Luo, R.; Merz, K. M., Jr.; Onufriev, A.; Simmerling, C.; Wang, B.; Woods, R.

J. The Amber biomolecular simulation programs. *J. Comput. Chem.* **2005**, *26*, 1668−1688.
(38) Chellaiah, A. T.; McEwen, D. G.; Werner, S.; Xu, J.; Ornitz, D. M. Fibroblast growth factor receptor (FGFR) 3. Alternative splicing in immunoglobulin-like domain III creates a receptor highly specific for acidic FGF/FGF-1. *J. Biol. Chem.* **1994**, *269*, 11620−11627.
(39) Yeh, B. K.; Eliseenkova, A. V.; Plotnikov, A. N.; Green, D.; Pinnell, J.; Polat, T.; Gritli-Linde, A.; Linhardt, R. J.; Mohammadi, M. Structural basis for activation of fibroblast growth factor signaling by sucrose octasulfate. *Mol. Cell. Biol.* **2002**, *22*, 7184−7192.
(40) Ibrahimi, O. A.; Yeh, B. K.; Eliseenkova, A. V.; Zhang, F.; Olsen, S. K.; Igarashi, M.; Aaronson, S. A.; Linhardt, R. J.; Mohammadi, M. Analysis of mutations in fibroblast growth factor (FGF) and a pathogenic mutation in FGF receptor (FGFR) provides direct evidence for the symmetric two-end model for FGFR dimerization. *Mol. Cell. Biol.* **2005**, *25*, 671−684.